Biotechnology Journal

DOI 10.1002/biot.201000159

Biotechnol. J. 2010, 5, 726–738

Research Article

Genome-scale metabolic modeling of a clostridial co-culture for consolidated bioprocessing

Fahimeh Salimi, Kai Zhuang and Radhakrishnan Mahadevan

Department of Chemical Engineering and Applied Chemistry, University of Toronto, Toronto, ON, Canada

An alternative consolidated bioprocessing approach is the use of a co-culture containing cellulolytic and solventogenic clostridia. It has been demonstrated that the rate of cellulose utilization in the co-culture of *Clostridium acetobutylicum* and *Clostridium cellulolyticum* is improved compared to the mono-culture of *C. cellulolyticum*, suggesting the presence of syntrophy between these two species. However, the metabolic interactions in the co-culture are not well understood. To understand the metabolic interactions in the co-culture, we developed a genome-scale metabolic model of *C. cellulolyticum* comprising of 431 genes, 621 reactions, and 603 metabolites. The *C. cellulolyticum* model can successfully predict the chemostat growth and byproduct secretion with cellulose as the substrate. However, a growth arrest phenomenon, which occurs in batch cultures of *C. cellulolyticum* at cellulose concentrations higher than 6.7 g/L, cannot be predicted by dynamic flux balance analysis due to the lack of understanding of the underlying mechanism. These genome-scale metabolic models of the pure cultures have also been integrated using a community modeling framework to develop a dynamic model of metabolic interactions in the co-culture. Co-culture simulations suggest that cellobiose inhibition cannot be the main factor that is responsible for improved cellulose utilization relative to mono-culture of *C. cellulolyticum*.

Received 30 April 2010
Revised 25 June 2010
Accepted 27 June 2010

Supporting information available online

Keywords: Clostridial co-culture · *Clostridium acetobutylicum* · *Clostridium cellulolyticum* · Genome-scale metabolic modeling · Systems biology

1 Introduction

In consolidated bioprocessing (CBP), all four biological steps involved in the conversion of cellulosic biomass, which includes production of saccharolytic enzymes, the hydrolysis of the polysaccharides present in pre-treated biomass, and fermentation of hexose and pentose sugars present in the hydrolyzate to desired products occur in one bioreactor using a single microorganism or a microbial consortium without the external addition of saccharolytic enzymes [1]. CBP has been proposed to decrease the product cost by eliminating some substrate costs, as well as utility, capital and other costs related to the cellulase production stage. However, microorganisms with both rapid conversion of cellulose and high-titer product formation capabilities required for CBP do not currently exist and need to be developed [2]. Current strategies for this purpose include the native strategy that improves the product formation capabilities, such as yield and titer in natural cellulolytic microorganisms, while the recombinant strategy involves engineering non- cellulolytic organisms with high product yields so that they will express heterologous cellulase and be able to utilize cellulose [2].

Clostridia are among the metabolically diverse group of bacteria and include both cellulolytic and solventogenic members. This metabolic diversity motivates an alternative method for the production of biobutanol from cellulosic biomass in a CBP ap-

Correspondence: Professor Radhakrishnan Mahadevan, Department of Chemical Engineering and Applied Chemistry, University of Toronto, 200 College Street, Toronto, ON, M5S 2E6 Canada
E-mail: krishna.mahadevan@utoronto.ca

Abbreviations: CBP, consolidated bioprocessing; **DMMM**, dynamic multi-species metabolic modeling; **FBA**, flux balance analysis; **FVA**, lux variability analysis; **GAM**, growth-associated maintenance energy; **GPR**, gene-protein reaction; **LDH**, lactate dehydrogenase; **PFO**,pyruvate-ferredoxin oxidoreductase

proach using a mesophilic clostridial co-culture. *Clostridium acetobutylicum* shows an effective capability to ferment hemicellulose-derived sugars as well as cellulose-derived sugars such as cellobiose, mannose, arabinose, xylose, glucose, and galactose, to acetone, butanol, and ethanol [3, 4]; so the co-culture of this bacterial species with a mesophilic cellulose-degrading bacterium can be an alternative option for CBP.

A simplified scheme of the clostridial co-culture fermentation on cellulose is presented in Fig. 1. *C. acetobutylicum* is a Gram-positive, solvent-producing, anaerobic bacterium that is able to convert a variety of sugars to organic acids and solvents. In a typical fermentation of this bacterium two distinct phases are observed; in the acidogenic phase, the bacterium grows rapidly and produces acetate, butyrate, and hydrogen, whereas in the stationary growth phase, the metabolic shift to solventogenesis takes place [5]. *Clostridium cellulolyticum*, which is cellulolytic mesophilic bacterium, synthesizes cellulosome (an extracellular multi-enzymatic complex), and degrades cellulose to glucose and soluble cellodextrins (mainly cellobiose) with the use of this cellulosome. This extracellular complex comprises a variety of cellulases, hemicellulase, and pectinase, which are arranged on a protein scaffold [6, 7]. The cellulosomes are located on the cell surface and facilitate both cell adhesion and cellulolytic activity on the cellulose fibers. However, in comparison to *Clostridium thermocellum*, the cellulosome of *C. cellulolyticum* is smaller and less complex [8].

The co-culture of *C. cellulolyticum* with *C. acetobutylicum* has been studied previously, and it has been shown that cellulolytic activity is the limiting factor in the co-culture fermentation since most of the cellulase activity products are consumed by *C. acetobutylicum*. The fermentation products are mainly butyric acid along with butanol, acetic acid and ethanol, and the lack of glucose, which is required for solvent production due to low cellulolytic activity, was hypothesized to be the reason for acid accumulation [5, 9]. Furthermore, three times more cellulosic material was degraded in the co-culture compared to the mono-culture of *C. cellulolyticum*, due to the utilization of cellulase activity products and the elimination of their repressive effects [10], suggesting the presence of syntrophy between these two species. Hence, the analysis of this effect can be valuable for optimizing the rate of cellulosic material degradation.

Limited growth and catabolic activity on cellulose is the common characteristic of the currently known cellulolytic bacteria [11]. Improving the cellulolytic and catabolic activity of *C. cellulolyticum* by metabolic engineering [12] can facilitate the shift of co-culture metabolism to the solventogenic phase. However, it has been demonstrated that the central metabolism of *C. cellulolyticum*, rather than the cel-

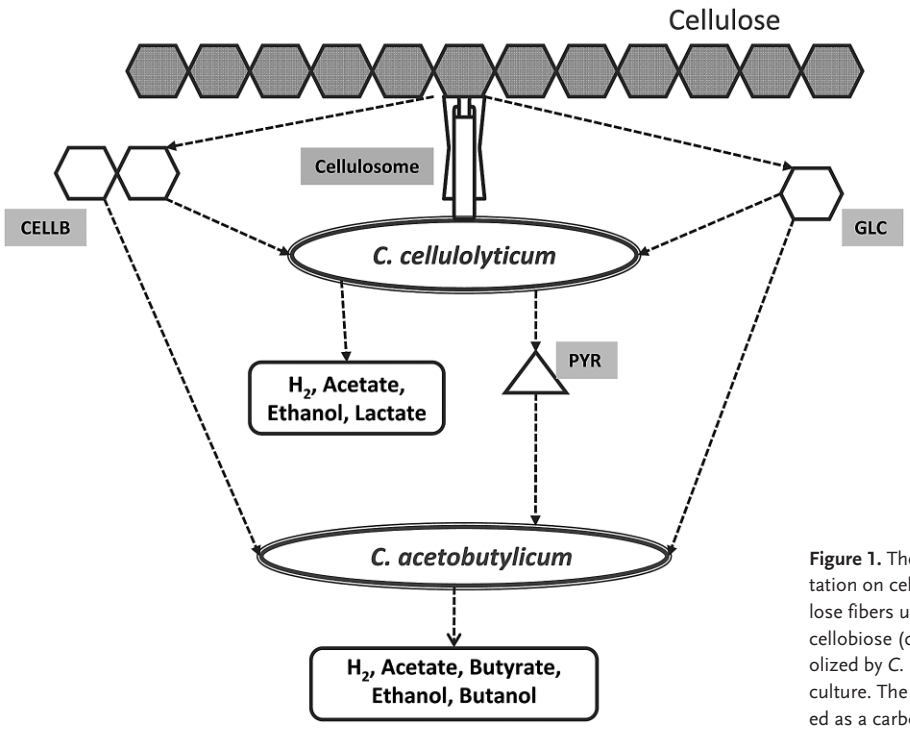

Figure 1. The scheme of the clostridial co-culture fermentation on cellulose. *C. cellulolyticum* adheres to the cellulose fibers using cellulosome and hydrolyzes cellulose to cellobiose (cellb) and glucose (glc), which can be metabolized by *C. cellulolyticum* and *C. acetobutylicum* in the co-culture. The produced pyruvate (pyr) can also be fermented as a carbon source by *C. acetobutylicum*.

lulose hydrolysis rate, is the limiting step in cellulose metabolism; therefore, improvement of *C. cellulolyticum* metabolism, which is not adapted to high catabolic rates, instead of the catalytic activity of the cellulosome is critical to improve its cellulolytic activity [11, 12]. Therefore, genome-scale metabolic modeling of *C. cellulolyticum* metabolism can provide an improved understanding of the bottleneck pathways and facilitate the improvement of this metabolic and cellulolytic activity using *in silico* generated hypotheses that can be tested experimentally. Furthermore, developing a genome-scale model of metabolism in this co-culture can assist in designing strategies for improving the yield and productivity of bioproducts via CBP.

Lee *et al*. [13] have reconstructed a genome-scale metabolic model of *C. acetobutylicum* with 11.2% ORF coverage, and applied this model to predict the metabolic behavior in acidogenic and solventogenic phases using flux balance analysis (FBA). Senger *et al*. [14, 15] have also presented another genome-scale metabolic model of *C. acetobutylicum* with 12.6% ORF coverage, and applied a genetic algorithm to derive a constraint based on the specific proton flux state to further restrict the solution space in FBA, and predict the pH of the batch culture during the acidogenic phase.

In this study, we present the genome-scale metabolic model of *C. cellulolyticum* H10, which comprises 431 genes, 621 reactions, 603 metabolites, and covers 12% of ORFs. Also, we developed an updated genome-scale metabolic model of *C. acetobutylicum* ATCC824, which consists of 700 genes, 712 reactions, and 679 metabolites, covering 16.3% of ORFs, and is more comprehensive compared to two other existing models. These metabolic networks were used as platforms for simulating phenotypes using the constraint-based modeling approach. The *C. cellulolyticum* model (*i*FS431) was able to predict the physiology during growth in the presence of cellulose and cellobiose. These models were used to develop a model of co-culture metabolism by combining these metabolic models of the pure cultures using the dynamic multi-species metabolic modeling (DMMM) framework (Zhuang *et al*., in press, see supplementary information). This co-culture model was used to analyze the integrated physiology of this co-culture, and the results showed that at high cellulose concentrations, the model is not able to capture the *C. cellulolyticum* growth arrest, suggesting that cellobiose inhibition removal by *C. acetobutylicum* is not the main factor that improves cellulose degradation in the co-culture. Further investigation to understanding the mechanism behind this growth arrest is required for improving the model predictions at high cellulose concentrations as well as predictions of the co-culture physiology.

2 Materials and methods

2.1 *C. acetobutylicum* and *C. cellulolyticum* metabolic network reconstructions

The automatically annotated genome sequence of *C. acetobutylicum* ATCC824 was downloaded from TIGR-CMR database (http://www.tigr.org/) and was used as a framework for gene-protein-reaction (GPR) assignments. The 4.13-Mb-length genome sequence of ATCC824 [16] comprises 4273 ORFs, and the GPR assignments were mostly based on this genome annotation; in addition, the automated metabolic network of ATCC824, reconstructed using Pathway Tools software version 11.5 and MetaCyc version 11.1 (http://biocyc.org/biocyc-pgdb-list.shtml) were used for confirmation of GPR assignments or re-annotations after manual inspection.

The model was reconstructed manually based on the metabolic roles in the existing annotation, and biochemical databases such as KEGG (http://www.genome.jp/kegg/) and the enzyme nomenclature database were consulted for more information on pathways, metabolites, and enzymes (http://ca.expasy.org/enzyme/). Transport reactions were included in the network according to the transport protein information in KEGG and TransportDB (http://www.membranetransport.org/) databases as well as the available physiological data. The biomass synthesis equation of *C. acetobutylicum*, which includes 40 mmol ATP/g DCW/h as the growth-associated maintenance energy (GAM) [13, 14] was included in the network as a demand reaction. *C. cellulolyticum* H10 Metabolic network was reconstructed based on the genome annotation available on JGI database (http://www.jgi.doe.gov/) for GPR associations, and using the available literature and experimental data. To find the transporter genes in the *C. cellulolyticum* H10 genome reciprocal blast was conducted, where the entire amino acid sequences were blasted against the Transport Classification Database (http://www.tcdb.org/) at the cut-off e-value equal to 10^{-5}. The candidate orthologous genes then were assigned to the corresponding transport reactions. Non-growth associated maintenance (NGAM) for growth of *C. cellulolyticum* on cellobiose has been reported to be 2.2 mmol ATP/g DCW/hour and 2.9 mmol ATP/g DCW/h for growth on cellulose [17].

The MetaFluxNet® version 1.82 was the platform used for the model reconstructions

(http:// mbel.kaist.ac.kr/lab/mfn/), and the reconstructed network models were then exported to Systems Biology Markup Language models (SBML; http://sbml.org), for further analyses using COBRA toolbox [18] in MATLAB environment (The MathWorks™). The elementally and charge balanced reaction equations were mostly obtained from BIGG database (http://bigg.ucsd.edu/) and SimPheny™ database (Genomatica Inc. San Diego, CA, USA). The chemical composition and charge of some particular metabolites, which did not exist in the aforementioned databases, were determined using ACD/LogD Sol Suite version 11.0 (http://www.acdlabs.com/) at the physiological pH of 6.7 ,which is consistent with the intracellular pH of *C. acetobutylicum* [5]. Pathway completion and gap filling were done manually so that the networks produce ATP along with all biomass building blocks, including amino acids, solute pool, nucleotides, cofactors, lipids and polysaccharides, from available substrates in their defined growth media [6, 19]. The BLAST search using UniProt BLAST tool (http://www.uniprot.org/) was applied to assign predicted functions to some missing ORFs in the original annotations as well as some ORF re-annotations. The GPR assignments also were done using available literature data. Further network evaluation and pathway completion were done using the COBRA toolbox; however, network gaps in some poorly characterized pathways can exist even after performing the network evaluation step. Non-gene-associated reactions were added to fill the gaps or to meet the physiological requirements according to the available literature data manually and using FBA. These reactions are detailed in Table 2 of the supporting information. The biomass macromolecular compositions were assumed to be identical to the *Bacillus subtilis* [13, 20], where the composition of nucleotides, protein, lipids and trace elements, as well as the required polymerization energy, were adapted from the model developed by Lee *et al.* [13].

2.2 Flux balance analysis

Metabolic phenotypes can be predicted by calculating the flux distributions through the metabolic networks using constraint-based modeling [21–23]. The FBA is based on the mass conservation law for each metabolite in the network. Vallino *et al*. [24] have shown that the steady-state approximation of the metabolite concentrations is a valid approximation, where, due to the intracellular metabolite concentrations and rapid metabolic fluxes, the metabolic transients are very fast in comparison to the time constants of the cell growth. In FBA, the constraints are defined by the stoichiometry of metabolic reactions, and flux distributions that satisfy these constraints, in this underdetermined system, are derived by optimizing a particular objective function such as growth rate or ATP production [25]. Thus, solving the linear programming (LP) problem subject to all constraints will result in a specific set of steady-state fluxes, which maximizes the objective function as well. In the *C. acetobutylicum* network, an additional constraint is required due to the presence of cyclic acid uptake pathways [26]. This constraint relates the acetate and butyrate uptake rates based on the enzyme kinetics and selectivity data and metabolite concentrations. The butyrate and acetate concentrations were obtained from chemostat data [27]; $Rate_{butuptake}$ and $Rate_{acuptake}$ are the rate of butyrate and acetate uptake, and $C_{butyrate}$, $C_{acetate}$ are extracellular butyrate and acetate concentration.

$$\frac{Rate_{butuptake}}{Rate_{acuptake}} = 0.315\,\frac{C_{butyrate}}{C_{acetate}} \tag{1}$$

However, alternate flux distributions can be achieved, using the linear programming technique, under the same optimal condition and objective value [28]. These alternate flux distributions provide information on the existence of alternate or redundant pathways in the metabolic network. In flux variability analysis (FVA), the optimal objective value is calculated by FBA, and then each flux is maximized and minimized under the same FBA constraints as well as the fixed optimal objective value.

2.3 Co-culture model development

The scheme of cellulose fermentation by *clostridial* co-culture is illustrated in Fig. 1. *C. cellulolyticum* can attach to the cellulose fibrils via the carbohydrate binding domains of the cellulosome, which is an extracellular multi-enzymatic complex located on the cell surface of *C. cellulolyticum* [7]. Due to the cellulolytic activity of the cellulosome, soluble sugars are released where cellobiose is the major product of cellulose hydrolysis [6], and it has been shown that glucose constitutes 30% of the cellulose hydrolysis products [29]. So in this study, we assumed the following stoichiometry for the cellulase reaction that takes place in *C. cellulolyticum* extracellular compartment by means of the cellulosome complex in the model:

$$Gcell + 0.65\,H_2O \rightarrow 0.35\,Cellb + 0.3\,glc \tag{2}$$

The co-culture system dynamics can be described using the following Eqs. (3–11), which are based on

the DMMM framework that is described in supplementary information part 1. The Michaelis-Menten kinetic parameters of cellulose solubilization and metabolism by *C. cellulolyticum* have been reported previously, where v_{max} is 2.91 mmol/g DCW/h [30], and K_m is equal to 0.8 g hexose equivalent/L [29]. It has been assumed that cellobiose inhibits the function of *C. cellulolyticum* cellulosome through a competitive inhibitory mechanism, similar to that demonstrated for *C. thermocellum* cellulosome [31]; the K_i value for competitive inhibition of endogluconase A component of the cellulosome is equal to 11 mM [32], and the K_i value of about 2 mM has been reported for *C. thermocellum* cellulosome [31].

$$V_{cellulase} = \frac{v_{\max} \cdot C_{Gcell}}{(1 + \frac{C_{cellb}}{k_i}).\, k_m + C_{Gcell}} \quad (3)$$

$$\frac{dC_{Gcell}}{dt} = -V_{cellulase}.\, X^{cc} \quad (4)$$

$$\frac{dC_{cellb}}{dt} = 0.35\, V_{cellulase}\, X^{cc} - V^{ca}_{cellb}\, X^{ca} - V^{cc}_{cellb}\, X^{cc} \quad (5)$$

$$\frac{dC_{glc}}{dt} = -\, V^{ca}_{glc}\, X^{ca} - V^{cc}_{glc}\, X^{cc} + 0.3\, V_{cellulase} \quad (6)$$

$$\frac{dC_{pyr}}{dt} = V^{cc}_{pyr}\, X^{cc} - V^{ca}_{pyr}\, X^{ca} \quad (7)$$

$$\frac{dX^{ca}}{dt} = \mu^{ca}\, X^{ca} \quad (8)$$

$$\frac{dX^{cc}}{dt} = \mu^{cc}\, X^{cc} \quad (9)$$

$$\text{Max } \mu^{ca} \quad (10)$$
$$\text{Subject to: } S^{ca}.\, V^{ca} = 0$$
$$V^{ca}_{glc} \le \frac{15.1\, C_{glc}}{3.56 + C_{glc}},\ V^{ca}_{cellb} \le \frac{2.47\, C_{cellb}}{1 + C_{cellb}},$$
$$V^{ca}_{pyr} \le \frac{5.91\, C_{pyr}}{1 + C_{pyr}},\ V^{ca}_{lac} \le \frac{40.2\, C_{lac}}{1.1 + C_{lac}},$$
$$V^{ca}_{ac} \le \frac{18.6\, C_{ac}}{1.4 + C_{ac}},$$

$$\text{Max } \mu^{cc} \quad (11)$$
$$\text{Subject to: } S^{cc}.\, V^{cc} = 0$$
$$V^{cc}_{glc} \le \frac{6.01\, C_{glc}}{20.22 + C_{glc}},\ V^{cc}_{cellb} \le \frac{5.01\, C_{cellb}}{20.22 + C_{cellb}}$$

Where C_{Gcell}, C_{cellb}, C_{glc}, C_{pyr}, C_{ac}, C_{lac} are cellulose, cellobiose, glucose, pyruvate, acetate and lactate concentrations, V is reaction rate obtained from FBA, and X^{ca} and X^{cc} are the *C. acetobutylicum* and *C. cellulolyticum* biomass concentrations. Kinetic data for *C. cellulolyticum* growth on cellobiose [17, 33] and glucose [34], and *C. acetobutylicum* growth on cellobiose [35], glucose [36, 37], pyruvate [38], acetate and lactate [39] were incorporated into the constraints. For modeling cellulose fermentation in batch and the co-culture, the upper limit of cellobiose uptake rate has been set to 0.76 mmol/g DCW/h to fit the experimental data [30]. Hence, μ^{ca} and μ^{cc} were obtained by solving the FBA problem for each species in Eqs. (10, 11), using maximization of growth rates as the objective functions, and the integration of these ODEs was performed using established methods in MATLAB [40].

3 Results and discussion

3.1 *C. cellulolyticum* metabolic network analysis

3.1.1 Central metabolism and energetics

The genomic features and specifications of *C. cellulolyticum* H10 (*i*FS431) metabolic network are shown in Fig. 2. Aligning *C. cellulolyticum* and *C. acetobutylicum* genomes using reciprocal BLAST at e-value cut-off of 10^{-2} suggests the existence of 1142 putative orthologous genes between these two species out of which 180 are currently present in the *C. acetobutylicum* metabolic network. The *i*FS431 network includes 603 metabolites, 621 reactions associated to 431 genes, and 68 reactions have been added as non-gene-associated reactions to fill

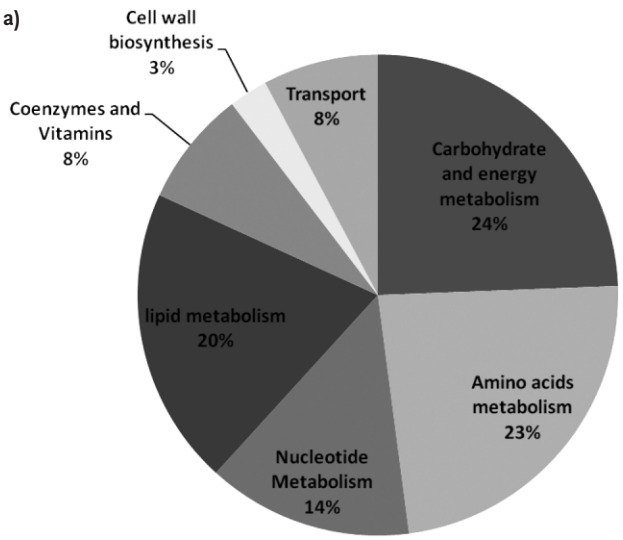

Figure 2. (a) Distribution of reactions in *C. cellulolyticum* metabolic network, and (b) the genomic features and specifications of *C. cellulolyticum* H10 metabolic network.

Figure 2b. Distribution of reactions in *C. cellulolyticum* metabolic network and the genomic features and specifications of *C. cellulolyticum* H10 metabolic network.

Characteristic	Quantity
The genome sequence length	4.1 Mb
Number of protein coding gene	3575
Number of genes included in the reconstructed network	431
ORF coverage (%)	12
The calculated number of orthologs among *C. acetobutylicum* and *C. cellulolyticum*	1148
The calculated number of orthologous genes which are existing in *C. acetobutylicum* model	180
Reactions/Metabolites	
Total number of model reactions	621
Gene associated reactions	513
Non- Gene associated reactions	71
Exchange reactions	37
Transport reactions	45
Total number of metabolites	603
Number of extracellular metabolites	46

the gaps or to meet the physiological requirements according to the available literature data [6]. This reconstruction is mainly based on the genome annotation available on JGI database. The TCA cycle and central metabolism pathways of *C. cellulolyticum* has not been characterized yet; however, this species is capable of producing succinate [34]. Therefore, succinate dehydrogenase is included in the model as a non-gene-associated reaction in the TCA cycle. Like *C. acetobutylicum*, the TCA cycle of *C. cellulolyticum* also seems to be bifurcated and it lacks succinate CoA ligase.

C. cellulolyticum degrades cellulose to glucose and soluble cellodextrins (mainly cellobiose) using its extracellular cellulosome. It has been suggested that the bioenergetics cost of cellodextrin transport is independent of the cellodextrin degree of polymerization [1], and for *C. cellulolyticum* 2 mol ATP is consumed per mole of each substrate transported through ABC transport system. The energetics cost of cellulosome biosynthesis has been included in the GAM value. Furthermore, there is an ATP gain associated with phosphorylitic cleavage of the cellodextrins (EC 2.4.1.20, EC 2.4.1.49), which can explain the higher biomass yield on cellobiose compared to glucose [1]. This higher yield is also predicted by the model. GAM was estimated using the available chemostat data [6] by minimizing the error between the model-predicted growth rate and the experimental data at various dilution rates on cellobiose, as shown in Fig. 3e. The estimated GAM value of 15 mmol ATP/g DCW/h was included in the biomass synthesis equation (see supplementary Table 1).

3.1.2 Analysis of byproduct secretion patterns in C. cellulolyticum during growth on cellobiose

The FBA was used to simulate the flux distributions in the reconstructed network in continuous cultures of *C. cellulolyticum* on cellobiose and cellulose [6, 17]. The maximization of growth rate was selected as the objective function, and the results of FBA for the growth on cellobiose are shown in Fig. 3d. The growth simulation on cellobiose demonstrates that acetate formation rate is significantly higher than the experimental data. *C. cellulolyticum* is a fermentative anaerobe and produces energy through the acetate formation pathway. To investigate the reason for high acetate flux and the presence of futile cycles, FVA on the acetate formation pathway under the same conditions and predicted growth rate of 0.116/h were conducted. The FVA showed that, for this growth rate, the minimum required ATP formation and acetate flux is 4.49 mmol/g DCW/h and rejects the presence of futile cycles. Another explanation for this can be the existence of alternate energy production pathways in *C. cellulolyticum*, as it has been shown recently that this genome encodes an energy-converting [NiFe] hydrogenase [41] that can couple the exergonic hydrogen formation reaction to the formation of a proton or sodium-ion motive force and energy conservation through oxidative level phosphorylation [42].

In addition, the model did not predict pyruvate formation, although it has been observed that pyruvate is produced at high dilution rates or carbon fluxes [12], and it has been suggested that limited pyruvate-ferredoxin oxidoreductase (PFO) activity, which cannot support high pyruvate flow, is the reason of this pyruvate overflow [6]. Furthermore, high pyruvate affinity of PFO (k_m=0.57 mM), as well as low pyruvate affinity of lactate dehydrogenase (LDH, k_m=4.5 mM), can explain the intracellular pyruvate accumulation and overflow [6]. Also, as shown in Fig. 3a, simulation of the *C. cellulolyticum* metabolism without any constraint on the LDH and PFO, at high cellobiose uptake rate (1.86 mmol/g DCW/h) showed that pyruvate will not be produced if there is no capacity constraint on these two reactions. Therefore, the upper bound for the LDH flux was set to the maximum observed lactate production rate, which is 0.5 mmol/g DCW/h [6], and by minimizing the error in predicted pyruvate formation rate , the upper bound for the flux through PFO was found to be 5.45 mmol/g DCW/h. The constraint on hydrogen formation flux has been set to $q_{H2} = 4q_{cellb}$ based on the fermentation

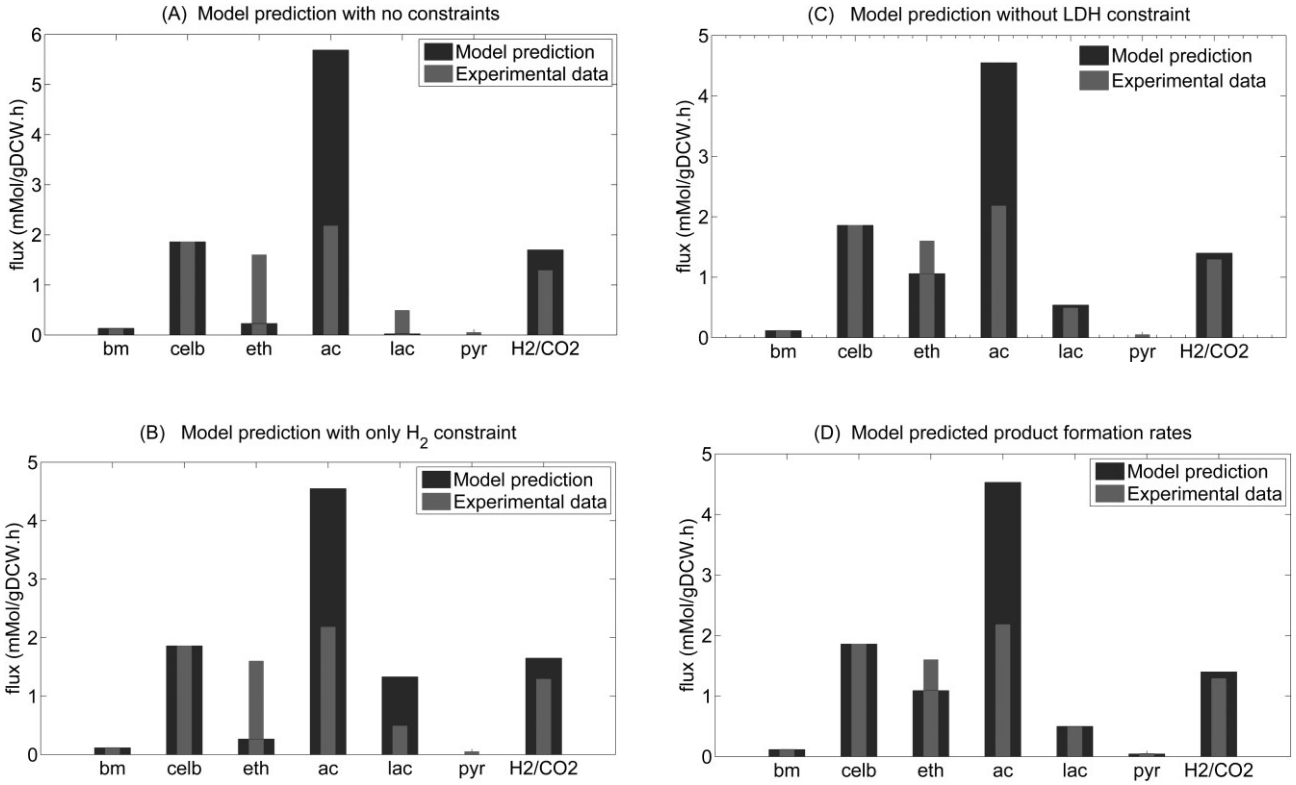

Figure 3. Model predicted metabolism of *C. cellulolyticum* in chemostat culture on cellobiose. (a) Model predicted cellobiose metabolism with no constraint on H_2 formation, LDH and PFO pathways; (b) model predicted cellobiose metabolism with no constraint on LDH and PFO pathways; (c) model predicted cellobiose metabolism with no constraint on LDH pathway; (d) model predicted product formation rates of *C. cellulolyticum* on cellobiose, D=0.12/h, and comparison with the experimental data [6]; (e) goodness of fit for *C. cellulolyticum* growth rate data on cellobiose at various dilution rates [6] and GAM=15 mmol/g DCW/h; bm, celb, eth, ac, lac, pyr stand for biomass, cellobiose, ethanol, acetate, lactate and pyruvate.

stoichiometry [6], and simulation results with expression of pyruvate decarboxylase (PDC) pathway showed that PDC pathway will not be active unless there is a constraint on hydrogen formation rate. Furthermore, Figs. 3b and c show that removing these constraints on PFO, LDH and hydrogen produc-tion pathways decreases the model prediction accuracy.

3.1.3 Analysis of C. cellulolyticum growth physiology on cellulose

To validate the model prediction, which was calibrated using cellobiose growth data, we compared the model simulations with cellulose as the substrate with experimental data. Modeling results show that the *i*FS431 model is able to appropriately predict the cellulose metabolism, growth rates and product formation rates, as depicted in Figs. 4a and e. We used cellobiose growth data for prediction of the GAM energetics parameter, and then used this calibrated model to predict the cellulose growth data. However, due to the cellulosome synthesis cost, the GAM value for growth on cellulose could be higher. As this cost has not been considered in the model, which was calibrated on cellobiose, the model over-predicts the growth rates in the Fig. 4.The rate of acetate formation is higher when *C. cellulolyticum* H10 is growing on cellulose, while it has higher growth rate on the cellobiose; this discrepancy might be related to the ATP cost of cellulosome biosynthesis, which is higher for the growth on cellulose, and leads to more ATP formation via acetate production pathway. The acetate and ethanol formation rates are properly predicted by the model; however, lactate and pyruvate secretion rates, which are significantly less than for the cellobiose growth case, could not be captured by the model. The impact of imposing the constraints on PFO, LDH and hydrogen production pathways on the model prediction of cellulose metabolism are illustrated in Figs. 4b–d to support the presence of these constraints.

3.1.4 *Analysis of C. cellulolyticum batch growth on cellulose*

We also applied dynamic FBA (dFBA) [43] to model the metabolism of *C. cellulolyticum* in a batch culture on cellulose [44]. The results of this simulation with the initial cellulose concentration of 6.7 g/L and initial biomass concentration of 20 mg/L are shown in Fig. 5a. Under these conditions *C. cellulolyticum* degrades approximately 80% of the cellulose and shifts to its stationary growth phase before complete cellulose exhaustion, which is due to a growth arrest and is thought to be caused by the accumulation of an intracellular metabolite [45]. This intracellular growth arrest, which has been shown to happen when cellulose concentration is higher than 3.9 g/L, cannot be captured using FBA; how-

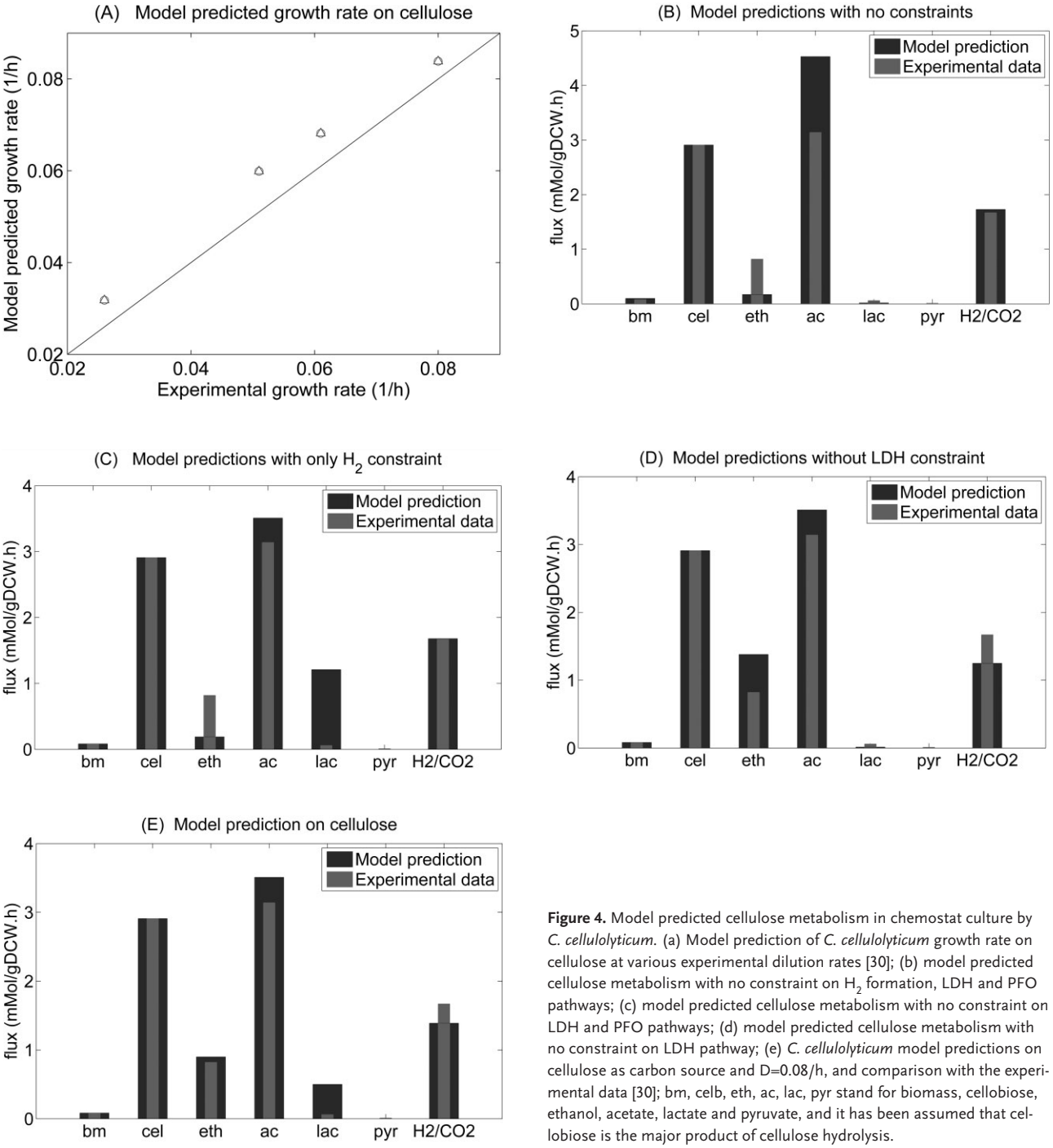

Figure 4. Model predicted cellulose metabolism in chemostat culture by *C. cellulolyticum*. (a) Model prediction of *C. cellulolyticum* growth rate on cellulose at various experimental dilution rates [30]; (b) model predicted cellulose metabolism with no constraint on H_2 formation, LDH and PFO pathways; (c) model predicted cellulose metabolism with no constraint on LDH and PFO pathways; (d) model predicted cellulose metabolism with no constraint on LDH pathway; (e) *C. cellulolyticum* model predictions on cellulose as carbon source and D=0.08/h, and comparison with the experimental data [30]; bm, celb, eth, ac, lac, pyr stand for biomass, cellobiose, ethanol, acetate, lactate and pyruvate, and it has been assumed that cellobiose is the major product of cellulose hydrolysis.

ever, in the exponential growth phase, the initial cellulose degradation and biomass growth patterns are well predicted by the model. Modeling this phenomenon requires the knowledge of the underlying growth arrest mechanism, and is a topic for further experimental studies. The results of dFBA for simulating the cellulose hydrolysis by *C. cellulolyticum* in a batch culture at an initial cellulose concentration of 3.9 g/L, where no growth arrest occurs, are depicted in Fig. 5b. The model is able to predict the cellulose hydrolysis accurately and there is a good agreement between the model prediction and the experimental data [45]; also, the predicted final biomass concentration of 364 mg/L is in accordance with the reported experimental value of 340 mg/L. Moreover, in batch cultures of *C. cellulolyticum*, glucose and cellobiose accumulation of up to 1.5 mM has been observed, which is also predicted by the model [44].

3.2 Genome-scale metabolic modeling of the co-culture and strategies for improving the co-culture metabolism

Cellulose metabolism mainly occurs when *C. cellulolyticum* is attached to the substrate [46], but in the batch cultures of *C. cellulolyticum* at high cellulose concentrations, cell growth terminates before substrate depletion [45]. Furthermore, it has been shown that re-inoculating a fresh culture of *C. cellulolyticum*, when substrate is not fully consumed, significantly improved the cellulose solubilization and biomass yield. This result indicates that the incomplete metabolism is not due to either the limitation of adhesion sites on cellulose fibers or product inhibition. At high cellulose concentrations, the likely explanation for the incomplete cellulose consumption is that the lack of control on carbon uptake flow and an imbalanced metabolism leads to the accumulation of intracellular metabolites and self-intoxication of the cells [11, 45].

Previous studies suggest that the cellobiose metabolic capacity is a limiting factor in the cellobiose metabolism by *C. cellulolyticum* since it is not able to metabolize high concentrations of cellobiose as the cells may not be able to efficiently control the cellobiose uptake [47]. The co-culture study of the *C. cellulolyticum* and *C. acetobutylicum* has shown improved cellulose fermentation, and the co-culture has been able to degrade entirely, a high amount of cellulose at a higher rate, compared to the monoculture of *C. cellulolyticum*. Hence, it can be hypothesized that cellobiose uptake by *C. acetobutylicum* improves the cellulose degradation process, and *C. acetobutylicum* can contribute in cellulose hydrolysis by preventing the cellobiose

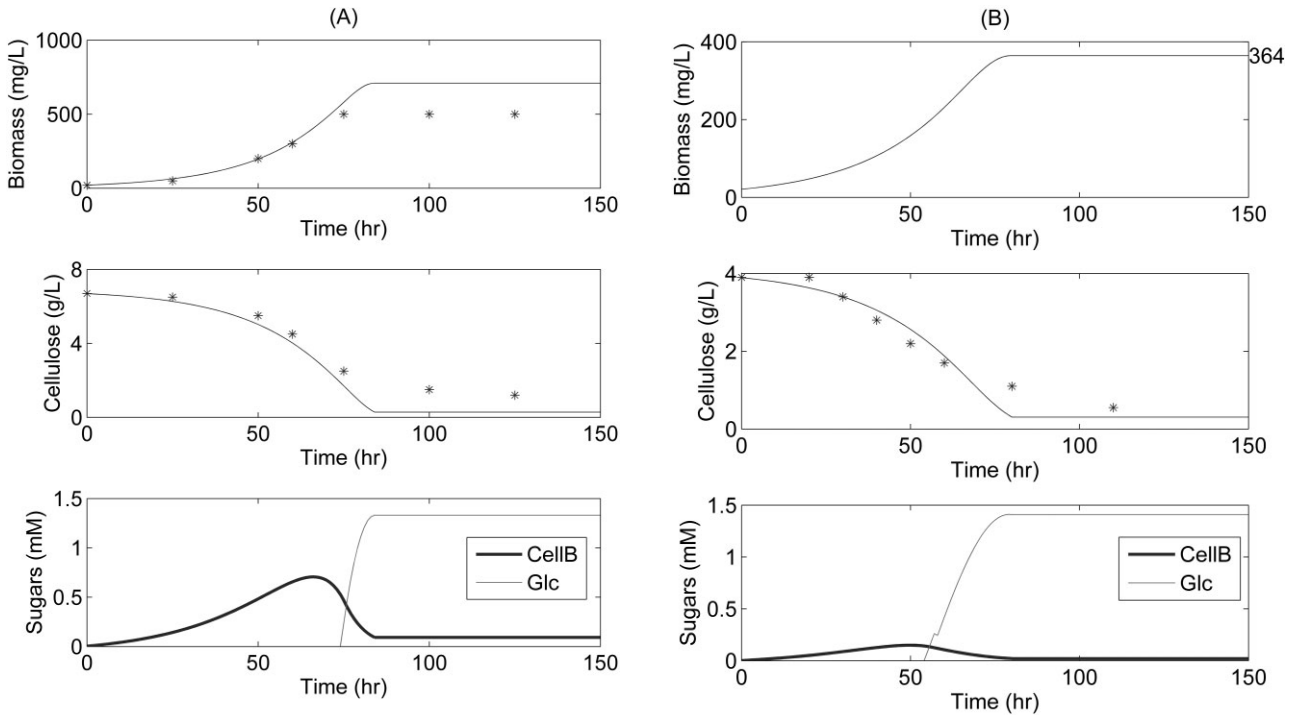

Figure 5. Model predicted metbolic profile of *C. cellulolyticum* in batch culture on cellulose. (a) Biomass and cellulose profiles are compared to the experimental data, at initial cellulose concentration of 6.7 g/L; (b) model predicted biomass and sugar profiles, and cellulose profile compared to the experimental data, at initial cellulose concentration of 3.9 g/L.

overflow, which is the major product of the cellulose hydrolysis, and the associated inhibitory effect on *C. cellulolyticum*. Therefore, it is crucial to know how the products of cellulose hydrolysis, cellobiose and glucose [29], impact the cellulosome activity and cellulose metabolism by the co-culture.

Previous reports have shown that the cellulosome of *C. thermocellum* is strongly inhibited by cellobiose, while glucose has an insignificant inhibitory effect. Furthermore, adding ß-glucosidase, which hydrolyses cellobiose, to the *C. thermocellum* culture has been shown to increase cellulose degradation rate and remove the adverse effects of cellobiose inhibition by hydrolyzing it to glucose. Cellobiose inhibits the function of *C. thermocellum* cellulosome through a competitive inhibitory mechanism [31]. So far, cellobiose inhibitory effect on the Cel5A, an endogluconase component of the *C. cellulolyticum* cellulosome has been established [32]. Furthermore, it has been shown that glucose has a significant derepressing effect on the production of cellulosome in *C. cellulolyticum,* and, in contrast to cellobiose, it does not have any inhibitory effect on its catalytic activity [48]. *C. acetobutylicum* has extracellular endogluconase and cellobiase activities during its growth on cellobiose [49], therefore improving the cellobiase activity and expression in *C. acetobutylicum*. This leads to the hydrolysis of cellobiose to glucose, and thus reducing the cellobiose inhibitory effect on the cellulosome activity can improve the cellulose degradation rate in this co-culture.

3.2.1 Analysis of co-culture for butanol production

Further interaction in this co-culture is related to the pyruvate metabolism; *C. cellulolyticum* typically secrets pyruvate as a result of its metabolic imbalance, and this can be metabolized by *C. acetobutylicum* in the co-culture. *C. cellulolyticum* secretes pyruvate as the result of a limited pyruvate

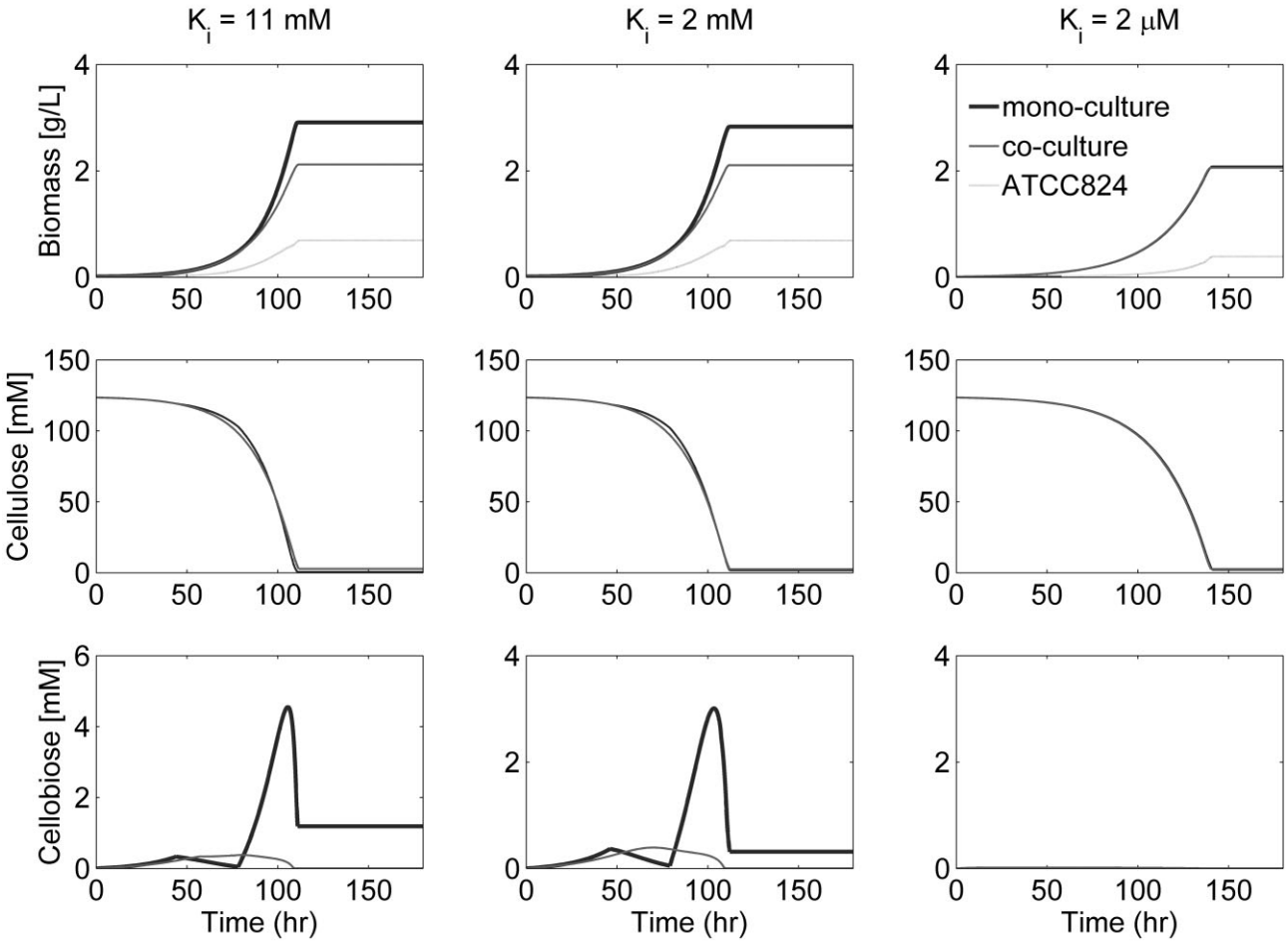

Figure 6. The kinetic profiles of the co-culture metabolism on cellulose, as predicted using the DMMM framework. *C. cellulolyticum* biomass concentration in the co-culture and mono-culture; *C. acetobutylicum* biomass concentration in the co-culture; cellulose hydrolysis profile in the co-culture and mono-culture; and cellobiose accumulation profiles in the co-culture and mono-culture under various cellobiose inhibition extents, at initial cellulose concentration of 20 g/L.

consumption rate and a comparatively higher carbon catabolism rate [47], while intracellular pyruvate accumulation could be the explanation for the growth arrest at high cellulose concentrations [12]. Also, it has been shown that providing *C. acetobutylicum* with pyruvate as the sole carbon source results in the growth and production of mainly acetate and butyrate [38]. The major products of pyruvate fermentation by *C. acetobutylicum* are acetate, butyrate and butanol, and neither acetate nor butyrate is reutilized. The effects of pyruvate on glucose fermentation by *C. acetobutylicum* have also been investigated before, and it has been shown that both substrates can be fermented simultaneously [50]. Therefore, a potential strategy for improving cellobiose metabolic capacity is through the redirection of the cellobiose toward secreted pyruvate, which can be later metabolized by *C. acetobutylicum*. In the study of co-culture fermentation of cellulose [9], high level of acids and a low titer of butanol have been reported. This observation can be explained by secretion of pyruvate by *C. cellulolyticum,* which affects the *C. acetobutylicum* metabolism and reduces the solvent formation, although the pyruvate formation in the co-culture was not measured. Moreover, it has been shown that addition of pyruvate to the glucose culture under pH-controlled condition represses the solventogenic pathways in *C. acetobutylicum* [50]. Based on this information, additional physiological and genetic manipulations are required to enhance the biobutanol production from cellulose by the co-culture.

Figure 6 depicts the model-predicted cellulose hydrolysis profiles in the co-culture, and these profiles have been compared to the simulated mono-culture profiles at various extents of cellobiose inhibition on cellulose hydrolysis rate. At a high cellulose concentration of 20 g/L, dFBA is not able to capture the *C. cellulolyticum* growth arrest; however, qualitative comparison of these two hypothetical profiles shows that, even at the K_i value of 2 mM, the cellobiose removal by *C. acetobutylicum* does not improve the rate of cellulose degradation in the co-culture. This result implies that cellobiose inhibition removal by *C. acetobutylicum* is not the main factor that improves cellulose degradation in the co-culture. The model prediction suggests that the concentration of cellobiose in the mono-culture is mostly less than 1 mM, which cannot significantly slow down the cellulose hydrolysis through the assumed competitive inhibition mechanism, and this K_i value of 2 mM is still too high for any significant inhibition due to cellobiose. Also, the experimental profiles of cellobiose and glucose concentrations have not been reported, and it is possible that a higher level of cellobiose accumulation takes place in the batch culture at this high cellulose concentration [45]. In addition, we have assumed a competitive inhibition mechanism for the modeling of cellobiose inhibitory effect on *C. cellulolyticum*, and it is possible that a different inhibitory mechanism affects the cellulosome activity. Hence, these simulations highlight the importance of the *C. cellulolyticum* cellulosome characterization. Further studies should investigate the underlying mechanism associated with the growth arrest phenomenon in *C. cellulolyticum* at high cellulose concentration.

4 Concluding remarks

Metabolic models have been used in the past to characterize *C. acetobutylicum* metabolism; however, FBA cannot predict the complex metabolism of *C. acetobutylicum* properly, and additional constraints are required to narrow down the solution space. Previously, specific proton flux states [15] were developed for this purpose. On the other hand, incorporating the regulatory network in the genome-scale model seems to be necessary for describing the metabolic shift from acidogenic to solventogenic phase [51]. In this work, we present the first genome-scale model of *C. cellulolyticum* metabolism that has been validated against the experimental data, and is able to predict the metabolism of *C. cellulolyticum* on cellulose and cellobiose. Furthermore, this model of *C. cellulolyticum* metabolism has been integrated with a *C. acetobutylicum* model to develop a genome-scale model of the clostridial co-culture metabolism. The results of our simulations suggest that (i) removal of cellobiose inhibition is not the main factor responsible for improved cellulose utilization in the co-culture, and (ii) *C. cellulolyticum* is primarily adapted to low carbon flow and availability [47]. These results also motivate the need for metabolic engineering strategies to enable *C. cellulolyticum* to handle high carbon flows. The inability of *C. cellulolyticum* to metabolize high concentrations of cellobiose [47] is a significant barrier to the development of commercial CBP process using clostridia. To overcome this limitation, there is a need to improve the cellobiose uptake capacity of *C. cellulolyticum,* assuming that the cellulosome function is not the limiting step [11]. Genome-scale models of *C. cellulolyticum* and the co-culture modeling framework, as presented here, will be valuable for further optimization of this co-culture for improved cellulose degradation and biobutanol production. This metabolic model of the co-culture can

also be easily extended to incorporate hemicellulose metabolism for growth on more complex cellulosic substrates.

Appendix

Nomenclature

μ^i	Specific growth rate of organism i (/h)
X^i	Biomass concentration of organism i (gDW/L)
C_j	Metabolite concentration of metabolite j (mmol)
C_{Gcell}	Cellulose concentration (mmol)
C_{cellb}	Cellobiose concentration (mmol)
C_{glc}	Glucose concentration (mmol)
C_{pyr}	Pyruvate concentration (mmol)
C_{ac}	Acetate concentration (mmol)
C_{lac}	Lactate concentration (mmol)
v_{max}	Maximum specific uptake rate of cellulose (mmol/g DW/h)
V_j^i	Specific uptake or secretion rate of metabolite j by the organism i (mmol/g DW/h)
V^i	Vector of reaction fluxes of organism i (mmol/g DW/h)
$V_{cellulase}$	Cellulose hydrolysis rate (mmol/gDW/h)
c_i	FBA objective vector of the i^{th} organism
S^i	Stoichiometric matrix of organism i
S_j^i	Sub-set of stoichiometric matrix of organism i corresponding to metabolite j
k_i	Cellobiose inhibition constant
k_m	Michaelis-Menten constant
$Rate_{butuptake}$	Rate of butyrate uptake by *C. acetobutylicum*
$Rate_{acuptake}$	Rate of acetate uptake by *C. acetobutylicum*
ub^i	Vector of upper-bound capacity constraints on the fluxes of organism i
lb^i	Vector of lower- bound capacity constraints on the fluxes of organism i

We acknowledge the funding from National Science and Engineering Research Council of Canada (NSERC), Canada's Agricultural Bioproducts Innovation Program (ABIP), Canadian Foundation for Innovation (CFI) and Ministry of Research and Innovation grants. Kai Zhuang was funded by the Office of Science (BER), U.S. Department of Energy (Cooperative Agreement No. DE-FC02-02ER63446 and Grant No. DE-FG02-07ER64367), and University of Toronto Open Fellowship to develop the DMMM framework.

The authors have declared no conflict of interest.

5 References

[1] Lynd, L. R., Weimer, P. J., Van Zyl, W. H., Pretorius, I. S., Microbial cellulose utilization: Fundamentals and biotechnology. *Microbiol. Mol. Biol. Rev.* 2002, *66*, 506–577.

[2] Lynd, L. R., Van Zyl, W. H., McBride, J. E., Laser, M., Consolidated bioprocessing of cellulosic biomass: An update. *Curr. Opin. Biotechnol.* 2005, *16*, 577–583.

[3] Yu, E. K. C., Deschatelets, L., Saddler, J. N., The bioconversion of wood hydrolyzates to butanol and butanediol. *Biotechnol. Lett.* 1984, *6*, 327–332.

[4] Fond, O., Engasser, J.-M., Matta-El-Amouri, G., Petitdemange, H., Acetone butanol fermentation on glucose and xylose. I. Regulation and kinetics in batch cultures. *Biotechnol. Bioeng.* 1986, *28*, 160–166.

[5] Jones, D. T., Woods, D. R., Acetone-butanol fermentation revisited. *Microbiol. Rev.* 1986, *50*, 484–524.

[6] Guedon, E., Payot, S., Desvaux, M., Petitdemange, H., Carbon and electron flow in *Clostridium cellulolyticum* grown in chemostat culture on synthetic medium. *J. Bacteriol.* 1999, *181*, 3262–3269.

[7] Desvaux, M., The cellulosome of *Clostridium cellulolyticum*. *Enzyme Microb. Technol.* 2005, *37*, 373–385.

[8] Felix, C. R., Ljungdahl, L. G., The cellulosome: The exocellular organelle of *Clostridium*. *Annu. Rev. Microbiol.* 1993, *47*, 791–819.

[9] Petitdemange, E., Fond, O., Caillet, F., A novel one step process for cellulose fermentation using mesophilic cellulolytic and glycolytic clostridia. *Biotechnol. Lett.* 1983, *5*, 119–124.

[10] Mitchell, W. J., Albasheri, K. A., Yazdanian, M., Factors affecting utilization of carbohydrates by clostridia. *FEMS Microbiol. Rev.* 1995, *17*, 317–329.

[11] Desvaux, M., *Clostridium cellulolyticum*: Model organism of mesophilic cellulolytic clostridia. *FEMS Microbiol. Rev.* 2005, *29*, 741–764.

[12] Guedon, E., Desvaux, M., Petitdemange, H., Improvement of cellulolytic properties of *Clostridium cellulolyticum* by metabolic engineering. *Appl. Eviron. Microbiol.* 2002, *68*, 53–58.

[13] Lee, J., Yun, H., Feist, A. M., Palsson, B. Ø., Lee, S. Y., Genome-scale reconstruction and in silico analysis of the *Clostridium acetobutylicum* ATCC 824 metabolic network. *Appl. Microbiol. Biotechnol.* 2008, *80*, 849–862.

[14] Senger, R. S., Papoutsakis, E. T., Genome-scale model for *Clostridium acetobutylicum*. Part I. Metabolic network resolution and analysis. *Biotechnol. Bioeng.* 2008, *101*, 1036–1052.

[15] Senger, R. S., Papoutsakis, E. T., Genome-scale model for *Clostridium acetobutylicum*. Part II. Development of specific proton flux states and numerically determined sub-systems. *Biotechnol. Bioeng.* 2008, *101*, 1053–1071.

[16] Nölling, J., Breton, G., Omelchenko, M. V., Makarova, K. S. *et al.*, Genome sequence and comparative analysis of the solvent-producing bacterium *Clostridium acetobutylicum*. *J. Bacteriol.* 2001, *183*, 4823–4838.

[17] Desvaux, M., Guedon, E., Petitdemange, H., Carbon flux distribution and kinetics of cellulose fermentation in steady-state continuous cultures of *Clostridium cellulolyticum* on a chemically defined medium. *J. Bacteriol.* 2001, *183*, 119–130.

[18] Becker, S. A., Feist, A. M., Mo, M. L., Hannum, G. *et al.*, Quantitative prediction of cellular metabolism with constraint-based models: The COBRA Toolbox. *Nat. Protoc.* 2007, *2*, 727–738.

[19] Monot, F., Martin, J. R., Petitdemange, H., Gay, R., Acetone and butanol production by *Clostridium acetobutylicum* in a synthetic medium. *Appl. Eviron. Microbiol.* 1982, *44*, 1318–1324.

[20] Oh, Y. K., Palsson, B. Ø., Park, S. M., Schilling, C. H., Mahadevan, R., Genome-scale reconstruction of metabolic network in *Bacillus subtilis* based on high-throughput phenotyping and gene essentiality data. *J. Biol. Chem.* 2007, *282*, 28791–28799.

[21] Feist, A. M., Herrgard, M. J., Thiele, I., Reed, J. L., Palsson, B. Ø., Reconstruction of biochemical networks in microorganisms. *Nat. Rev. Microbiol.* 2009, *7*, 129–143.

[22] Price, N. D., Reed, J. L., Palsson, B. Ø., Genome-scale models of microbial cells: Evaluating the consequences of constraints. *Nat. Rev. Microbiol.* 2004, *2*, 886–897.

[23] Henry, C. S., Broadbelt, L. J., Hatzimanikatis, V., Thermodynamics-based metabolic flux analysis. *Biophys. J.* 2007, *92*, 1792–1805.

[24] Vallino, J. J., Stephanopoulos, G., Metabolic flux distributions in *Corynebacterium glutamicum* during growth and lysine overproduction. *Biotechnol. Bioeng.* 1993, *41*, 633–646.

[25] Schilling, C. H., Edwards, J. S., Letscher, D., Palsson, B. Ø., Combining pathway analysis with flux balance analysis for the comprehensive study of metabolic systems. *Biotechnol. Bioeng.* 2000, *71*, 286–306.

[26] Desai, R. P., Nielsen, L. K., Papoutsakis, E. T., Stoichiometric modeling of *Clostridium acetobutylicum* fermentations with non-linear constraints. *J. Biotechnol.* 1999, *71*, 191–205.

[27] Meyer, C. L., Papoutsakis, E. T., Continuous and biomass recycle fermentations of *Clostridium acetobutylicum*. Part 1: ATP supply and demand determines product selectivity. *Bioprocess Eng.* 1989, *4*, 1–10.

[28] Mahadevan, R., Schilling, C. H., The effects of alternate optimal solutions in constraint-based genome-scale metabolic models. *Metab. Eng.* 2003, *5*, 264–276.

[29] Giallo, J., Gaudin, C., Belaich, J. P., Metabolism and solubilization of cellulose by *Clostridium cellulolyticum* H10. *Appl. Eviron. Microbiol.* 1985, *49*, 1216–1221.

[30] Desvaux, M., Guedon, E., Petitdemange, H., Kinetics and metabolism of cellulose degradation at high substrate concentrations in steady-state continuous cultures of *Clostridium cellulolyticum* on a chemically defined medium. *Appl. Eviron. Microbiol.* 2001, *67*, 3837–3845.

[31] Kruus, K., Andreacchi, A., Wang, W. K., Wu, J. H. D., Product inhibition of the recombinant CelS an exoglucanase component of the *Clostridium thermocellum* cellulosome. *Appl. Microbiol. Biotechnol.* 1995, *44*, 399–404.

[32] Fierobe, H. P., Gaudin, C., Belaich, A., Loutfi, M. *et al.*, Characterization of endoglucanase A from *Clostridium cellulolyticum*. *J. Bacteriol.* 1991, *173*, 7956–7962.

[33] Guedon, E., Payot, S., Desvaux, M., Petitdemange, H., Relationships between cellobiose catabolism, enzyme levels, and metabolic intermediates in *Clostridium cellulolyticum* grown in a synthetic medium. *Biotechnol. Bioeng.* 2000, *67*, 327–335.

[34] Giallo, J., Gaudin, C., Belaich, J. P., Metabolism of glucose and cellobiose by cellulolytic mesophilic *Clostridium* sp. strain H10. *Appl. Eviron. Microbiol.* 1983, *45*, 843–849.

[35] Lopez-Contreras, A. M., Martens, A. A., Szijarto, N., Mooibroek, H. *et al.*, Production by *clostridium Acetobutylicum* ATCC 824 of CelG, a cellulosomal glycoside hydrolase belonging to family 9. *Appl. Eviron. Microbiol.* 2003, *69*, 869–877.

[36] Yang, X., Tsao, G. T., Mathematical modeling of inhibition kinetics in acetone-butanol fermentation by *Clostridium acetobutylicum*. *Biotechnol. Prog.* 1994, *10*, 532–538.

[37] Houston, C. L. M., Papoutsakis, E. T., Continuous and biomass recycle fermentations of *Clostridium acetobutylicum*. Part 2: Novel patterns in energetics and product-formation kinetics. *Bioprocess Eng.* 1989, *4*, 49–55.

[38] Janati-Idrissi, R., Junelles, A. M., El Kanouni, A., Petitdemange, H., Gay, R., Pyruvate fermentation by *Clostridium acetobutylicum*. *Biochem.Cell Biol.* 1989, *67*, 735–739.

[39] Diez-Gonzalez, F., Russell, J. B., Hunter, J. B., The role of an NAD-independent lactate dehydrogenase and acetate in the utilization of lactate by *Clostridium acetobutylicum* strain P262. *Arch. Microbiol.* 1995, *164*, 36–42.

[40] Covert, M. W., Xiao, N., Chen, T. J., Karr, J. R., Integrating metabolic, transcriptional regulatory and signal transduction models in *Escherichia coli*. *Bioinformatics* 2008, *24*, 2044–2050.

[41] Calusinska, M., Happe, T., Joris, B, Wilmotte, A., The surprising diversity of clostridial hydrogenases: a comparative genomic perspective. *Microbiology* 2010, *156*, 1575–1588.

[42] Hedderich, R., Energy-converting [NiFe] hydrogenases from Archaea and Extremophiles: Ancestors of complex I. *J. Bioenerg. Biomembr.* 2004, *36*, 65–75.

[43] Mahadevan, R., Edwards, J. S., Doyle Iii, F. J., Dynamic flux balance analysis of diauxic growth in *Escherichia coli*. *Biophys. J.* 2002, *83*, 1331–1340.

[44] Desvaux, M., Guedeon, E., Petitdemange, H., Metabolic flux in cellulose batch and cellulosefed continuous cultures of *Clostridium cellulolyticum* in response to acidic environment. *Microbiology* 2001, *147*, 1461–1471.

[45] Desvaux, M., Guedon, E., Petitdemange, H., Cellulose catabolism by *Clostridium cellulolyticum* growing in batch culture on defined medium. *Appl. Eviron. Microbiol.* 2000, *66*, 2461–2470.

[46] Gelhaye, E., Gehin, A., Petitdemange, H., Colonization of crystalline cellulose by *Clostridium cellulolyticum* ATCC 35319. *Appl. Eviron. Microbiol.* 1993, *59*, 3154–3156.

[47] Guedon, E., Desvaux, M., Payot, S., Petitdemange, H., Growth inhibition of *Clostridium cellulolyticum* by an inefficiently regulated carbon flow. *Microbiology* 1999, *145*, 1831–1838.

[48] Petitdemange, E., Tchunden, T., Valles, S., Pirson, H. *et al.*, Effect of carbon sources on cellulase production by *Clostridium cellulolyticum*. *Biomass Bioenergy* 1992, *3*, 393–402.

[49] Lee, S. F., Forsberg, C. W., Gibbins, L. N., Cellulolytic activity of *Clostridium acetobutylicum*. *Appl. Eviron. Microbiol.* 1985, *50*, 220–228.

[50] Junelles, A. M., Janati-Idrissi, R., Petitdemange, H., Gay, R., Effect of pyruvate on glucose metabolism in *Clostridium acetobutylicum*. *Biochimie* 1987, *69*, 1183–1190.

[51] Covert, M. W., Schilling, C. H., Palsson, B. Ø., Regulation of gene expression in flux balance models of metabolism. *J. Theor. Biol.* 2001, *213*, 73–88.